Computers and Chemical Engineering 71 (2014) 323–330

Contents lists available at ScienceDirect

Computers and Chemical Engineering

journal homepage: www.elsevier.com/locate/compchemeng

Model predictive temperature tracking in crystal growth processes

Javad Abdollahi, Mojtaba Izadi, Stevan Dubljevic*

Department of Chemical and Materials Engineering, University of Alberta, Edmonton, Alberta, Canada T6G 2V4

ARTICLE INFO

Article history:
Received 5 April 2014
Received in revised form 6 July 2014
Accepted 6 September 2014
Available online 16 September 2014

Keywords:
Parabolic partial differential equation
Moving boundary domain
Czochralski crystal growth
Model predictive control
Reference trajectory tracking

ABSTRACT

The temperature gradients and distribution evolution within the crystal domain in Czochralski crystal growth process have important role in produced crystal's quality. Precise and tight regulation of temperature distribution and gradients is the most promising approach to ensure the crystal quality. In this work, the coupled crystal pulling dynamics and heat transfer models in Czochralski crystal growth with a time-varying boundary is considered. The moving boundary finite element method is used to obtain the optimal reference temperature trajectory associated with the reference crystal shape taking into account constraints on input and the temperature gradients. The obtained reference trajectory is used to implement a model predictive control strategy to track the reference temperature despite uncertainties in crystal domain geometry evolution and disturbances. Finally, the proposed method is implemented on a high fidelity finite element process model with non-planar interface and results are presented to validate the success of the proposed methodology.

1. Introduction

Single crystals, due to unique mechanical, physical and electrical properties are common materials in microelectronics, optoelectronics and structurally robust and high temperature resistant applications (Sinno and Brown, 1999; Sinno et al., 2000). The Czochralski (Cz) crystal growth process is the most common mass production process to produce single crystal. In Cz process, the solid crystal is grown from molten material (Si, Ga, etc), starting from a small crystal seed and slowly growing by solidification of material at the melt-crystal interface. Due to the high-tech nature of single crystal applications, the quality of the grown crystal is of crucial importance. The crystal quality is defined by physical properties of the produced crystal such as defects density and developed residual stresses in the crystal. These defects and residual stresses are caused by significant temperature gradients in the crystal and can be regulated by introducing a controller to limit possibly large temperature gradient fluctuations (see (Gevelber and Stephanopoulos, 1987).

In order to realize process regulation in CZ crystal growth process one needs process model. The Czochralski crystal growth process modeling requires a sophisticated model of melt fluid flow, thermal and heat transfer phenomena, solid-liquid interface and pulling dynamics. There are recent studies focusing on modeling and simulation of the coupled phenomena together (Cao et al., 2011; Demina and Kalaev, 2011). However for control purposes a simplified model of the phenomena of interest would suffice and usual assumptions are made to decouple specific processes to achieve a reduced order model as a basis for model based control synthesis. In the recent review on the automation of Czochralski crystal growth process (Winkler et al., 2013), both the classical and modern control realizations which are synthesized on the simplified process model description have been reported and critically accessed (Winkler et al., 2010a, 2010b). At present time, one can conclude that a successful controller synthesis relies on the interplay among feedback, feedforward control, the reference trajectory tracking and reconstruction of non directly measurable process states. Therefore, any controller realization is dependent on the quality of the model used in controller synthesis.

In particular, due to a specific feature of the Czochralski crystal growth process, the crystal shape undergoes time-varying changes which introduces moving boundaries to the parabolic partial differential equations (PDE) model of temperature evolution in the crystal growth process. Along this line, there are several works focusing on the model based controller design of parabolic PDE models with time-varying boundary domain, see Armaou and Christofides (2001a, 2001b), Rudolph et al. (2005). For example, Armaou and Christofides (2001a, 2001b) have reduced the 2-D heat transfer model on a rectangular domain of the crystal to a 1-D model and synthesized nonlinear controller for temperature regulation. Ng and Dubljevic (2012), Ng et al. (2013) studied optimal boundary control of the 2-D temperature model of the Cz crystal growth

* Corresponding author. Tel.: +1 780 248 1596; fax: +1 780 492 2881.
E-mail address: Stevan.Dubljevic@ualberta.ca (S. Dubljevic).

http://dx.doi.org/10.1016/j.compchemeng.2014.09.005
0098-1354/

process with moving boundaries which is coupled with the crystal pulling dynamics. In these contributions, a simplified geometry (e.g. 1-D or 2-D rectangular domain) is used for control synthesis, however in realistic operation of Cz process, the crystal growth starts from a small three dimensional irregularly shaped seed and grows to a boule with relatively small fluctuations in desired radius.

One of the main obstacles in producing high quality large boules of a grown crystal is the presence of thermal stresses during the crystal cooling. The thermal stresses result in crystal cracking and fracture in the crystal during the cooling process. The critical stresses in the crystal depend on the crystal temperature and are usually caused by temperature difference in radial direction (Gevelber and Stephanopoulos, 1987; Gevelber et al., 1988; Fang et al., 2008). Controlling or limiting these stresses are crucial to avoid crystal cracking and to ensure the crystal quality. The conventional method to control these stresses are to adjust the heater temperature in order to maintain the temperature distribution around desired levels, however for larger crystals this method is not successful. In particular, the conventional methods are usually realized as off-line configuration accompanied with large scale simulation studies. The modern control strategies are helpful for on-line temperature distribution control, however limitations associated with distributed temperature measurement realization, the infinite-dimensional nature of the heat transfer process, time-varying crystal boundaries, stringent performance requirements reflected in grown crystal quality and coupled pulling and heat transfer dynamics make the control implementation a challenging task. One of the modern control realizations capable of accounting for the aforementioned performance and process characteristics in explicit way is the model predictive control.

Model Predictive Control (MPC) strategies due to their practical and industrially appealing advantages attracted quite a few contributions in the area of Czochralski crystal growth and temperature control. For example,Lee et al. (2005) used the MPC to determine a feedforward trajectory for crystal growth control. Temperature distribution control in solid crystal and melt is also performed by Ng et al. (2013), Irizarry-Rivera and Seider (1997) where the main approach in these contributions is to use a reduced order model of the complex dynamical system to apply the MPC and ensure that desired performance objectives are satisfied. In Irizarry-Rivera and Seider (1997) work, the lumped models are considered for both the pulling dynamics and bulk heat transfer and then two different MPC are coupled to control the radius and pulling velocity. Although utilizing a more sophisticated model of the process would be more accurate and due to the improved performance recommended, the complexity and the computational efforts associated with more detailed models must be weighted against ability of these algorithms to be implemented on-line in real-time setting.

The control strategies have been previously developed to control the crystal radius (Gevelber and Stephanopoulos, 1987; Neubert and Winkler, 2012; Winkler et al., 2010a), pulling velocity (Winkler et al., 2010a; Lee et al., 2005), melt temperature (Irizarry-Rivera and Seider, 1997) and for stabilization of temperature distribution (Ng et al., 2013; Irizarry-Rivera and Seider, 1997; Armaou and Christofides, 2001a), however to the best of authors' knowledge, there are no control strategies developed for optimal temperature distribution tracking with the ultimate objective of reducing the dislocation concentration distribution in grown crystal. Motivated by this, the crystal growth practitioners would seek the control strategy which maximizes crystal cooling without inducing a significant dislocation generation.

In this work, a framework is provided for reference temperature profile tracking in the Czochralski crystal growth process in the presence of temperature distribution and gradient constraints which are directly linked to the quality of grown crystal. A predefined reference crystal shape evolution is used to calculate the optimal temperature trajectory. The reference trajectory is determined to achieve the maximum rate of crystal cooling and all constraints associated with temperature and gradient distributions are taken into account along with constraints on available actuator input. The moving boundary finite element model (FEM) of the conduction-convection thermal phenomena within the reference crystal shape is used to determine the optimal temperature distribution trajectory. Then the MPC is designed to track desired temperature distribution and satisfies stringent performance criteria.

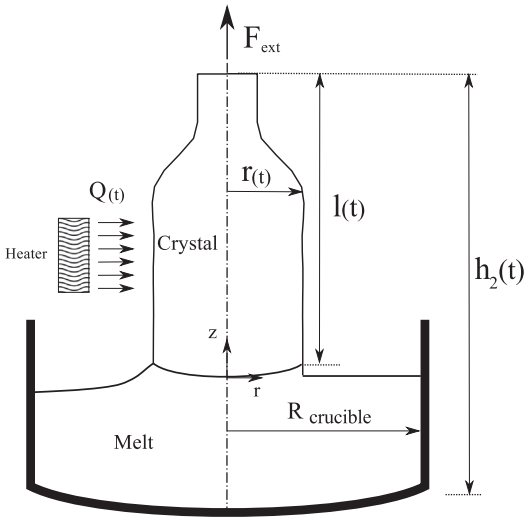

Fig. 1. Schematic of the Cz crystal growth process with the realistic geometry of the process given in the left figure side, and geometric simplifications and parameters given in the right figure side.

The organization of the paper is given as following: after Section 1, a brief description of the pulling dynamics, heat transfer model and thermal stresses are provided in Section 2. In the following sections the optimization and the MPC controller realizations are presented and followed by numerical results and discussion.

2. Heat transfer model on moving boundary domain

The solid crystal growth process model, that we considered in this work, consists of coupled crystal boule growth and heat transfer dynamics. In general, the crystal growth model dynamics depicts crystal radius and length evolution which determines the domain boundaries of heat transfer model. On the other hand, the crystal shape evolution is influenced by temperature distribution and thermal phenomena (see Fig. 3). This two-way coupling is reduced to one-way coupling model realization using a robust controller such that the influence of the temperature distribution on the crystal growth dynamics is considered as a parametric uncertainty in the crystal growth rate.

2.1. Crystal pulling dynamics model

The schematic of the crystal pulling dynamics along with the notations are presented in Fig. 1. The pulling dynamics model is derived assuming horizontal melt–solid interface (see Abdollahi et al. (2014), Abdollahi and Dubljevic (2013)). The pulling dynamics model is given by:

$$\begin{aligned}\dot{x}_1(t) &= x_2(t)\\ \dot{x}_2(t) &= \frac{2}{\rho_c x_3(t)}\left[F_{ext}(t) - \rho_c \pi C_{growth}\left(\frac{x_2(t)}{2} - \frac{C_{growth}}{R_{cruc.}^2}\right)\right] \qquad (1)\\ \dot{x}_3(t) &= \pi C_{growth}\end{aligned}$$

and the crystal radius at the interface, $R_{c.i.}(t)$, as the output is given as:

$$R_{c.i.}(t) = \sqrt{\frac{C_{growth}}{x_2(t)}} = \sqrt{\frac{C_{growth}}{\dot{l}(t)}} \tag{2}$$

where $x_1(t) = l(t)$, $x_2(t) = \dot{l}(t)$ and $x_3(t) = V_c(t)$ are the crystal length, growth velocity and the crystal volume, respectively. F_{ext}, C_{growth}, $R_{cruc.}$ and ρ_c are the puling force, volumetric crystal growth rate, crucible radius and the crystal density, respectively (see Fig. 1). The control objective is to regulate the crystal radius at a desired value, R_d, despite the parametric uncertainty. The controller is designed using input-output linearization of the pulling dynamics model, given by:

$$F_{ext}(t) = \rho\pi C_{growth}^2 \left(\frac{1}{2R_{c.i.}^2(t)} - \frac{1}{R_{cruc.}^2}\right) + K\rho\pi C_{growth}^2 \left(t + \frac{V_{c0}}{\pi C}\right) \frac{R_{c.i.}(t) - R_d}{R_{c.i.}^3(t)} \tag{3}$$

where K is the controller gain which is determined to stabilize the crystal radius at desired value considering the parametric uncertainty in the crystal growth rate $C_{nominal} - d(t) \le C_{growth} \le C_{nominal} + d(t)$. The range of K is given as:

$$K > \frac{\pi}{2V_{c0}C_{growth}^2} D(C_{growth} + D)(2C_{growth} + D) \tag{4}$$

where D is an upper limit for disturbance $d(t)$ and is assumed to have a lower and upper limit, $-C_{growth} < d(t) < D$. The lower limit corresponds to the case of crystallization not occurring and the upper bound, which represents fast crystallization, can be arbitrarily chosen.

The crystal radius is well regulated despite the uncertainty in the crystal growth rate due to the thermal disturbance introduced by $d(t)$. It is also known that the crystal growth rate is determined by heat transfer dynamics and temperature distribution in the crystal, melt and crystal-melt interface. Providing a robust control law with respect to growth rate, the radius control synthesis can be realized without considering detailed influence of thermal disturbance phenomena. This is an important point in considering the coupled thermal and pulling dynamics used for the control purposes. In other words, the bidirectional coupling can be effectively reduced by the robust feedback linearizing control to a one-directional coupling. In the ensuing section we provide the heat transfer PDE model with moving domain dynamics that is driven by the time-varying evolution of the $x_1(t)$-state in Eq. (1) and $R_{c.i.}(t)$ in Eq. (2).

2.2. Heat transfer model

In the Czochralski process, the heat transfer within the solid crystal is described by the conduction-convection PDE model given by Eq. (5) where convective terms are manifested by the boundaries movement velocity. The model is given as follows:

$$Pe\frac{\partial x(r,z,t)}{\partial t} = \nabla\cdot(k_r\nabla x(r,z,t)) - Pe\mathbf{V}(r,z,t)\cdot\nabla x(r,z,t) \tag{5}$$

where $x(r, z, t)$ is the scaled temperature within the crystal, ∇ is the spatial gradient operator in the cylindrical coordinate system, $Pe = \rho C_p v_0 R_{cruc.}/k_s$ is the Peclet number, v_0, $R_{cruc.}$, k_s and k_r are the nominal pulling velocity, crucible radius, regional thermal conductivity and conductivity ratio, respectively and $\mathbf{V}(r,z,t)$ is the velocity vector field over the entire crystal domain. The model is written as appropriately scaled time-varying temperature dynamics model where the temperature is scaled by solidification-melting temperature T_f as $x = (T - T_f)/T_f$, r and z are scaled with respect to crucible radius, while the time is scaled with respect to nominal pulling velocity $R_{cruc.}/v_0$ (Derby and Brown, 1987).

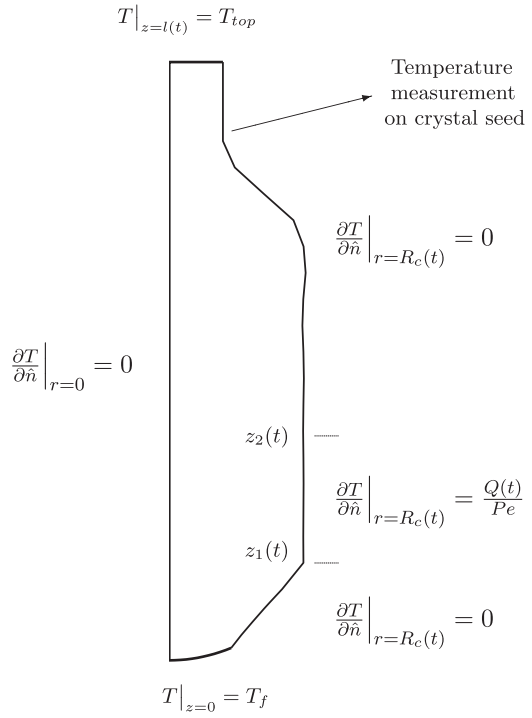

Fig. 2. Boundary conditions, actuation interval and measurement point.

At the melt–solid interface (see Fig. 2), as solidification happens, the temperature is assumed to be at melting point temperature ($x|_{z=0} = 0$) and constant temperature is considered at the top of the crystal. In order to have closer thermal behaviour to real operating conditions, Dirichlet boundary condition is considered at the top of the crystal and it is considered to be equal to $T_{top} = 850\,^{\circ}\mathrm{C}$ (taken from the experimental results of Sinno et al. (2000)).

$$x|_{z=0} = 0; \qquad x|_{z=l(t)} = x_{top} \tag{6}$$

The control actuation is provided by a heater which is installed along axial crystal direction in interval at the crystal surface and provides radial heat flux rate of $Q(t)$. The corresponding boundary condition is given by:

$$\frac{\partial x}{\partial \hat{n}}|_{r=R_c(z),z_1(t)<z<z_2(t)} = \frac{Q(t)}{Pe} \tag{7}$$

where $Q(t)$ is the heat flux provided by the local heater. $R_c(z)$ is the crystal radius at height z and $z_1(t)$ and $z_2(t)$ indicate the spatial interval where the heater is placed. Note that the heater location varies with respect to the crystal as it grows. R_c, $l(t)$, $z_1(t)$ and $z_2(t)$ are determined from the pulling dynamics model given by Eqs. (1) and (2). Moreover, the process is axisymmetric (no flux at $r = 0$) and at all other boundaries, the zero flux boundary condition is assumed (see Fig. 2).

$$\frac{\partial x}{\partial r}|_{r=0} = 0; \quad \frac{\partial x}{\partial \hat{n}}|_{r=R_c(z),z<z_1(t)} = 0; \quad \frac{\partial x}{\partial \hat{n}}|_{r=R_c(z),z>z_2(t)} = 0 \tag{8}$$

The boundary velocity along the radial direction is neglected and therefore, the temperature evolution is rewritten as follows:

$$\frac{\partial x}{\partial t} = \frac{1}{r}\frac{\partial}{\partial r}\left(k_0 r\frac{\partial x}{\partial r}\right) + k_0\frac{\partial^2 x}{\partial z^2} - V_z(t)\frac{\partial x}{\partial z} \tag{9}$$

where $k_0 = k_r/Pe$ and $V_z(t)$ is the bulk movement velocity along the axial direction. The temperature evolution model of the grown

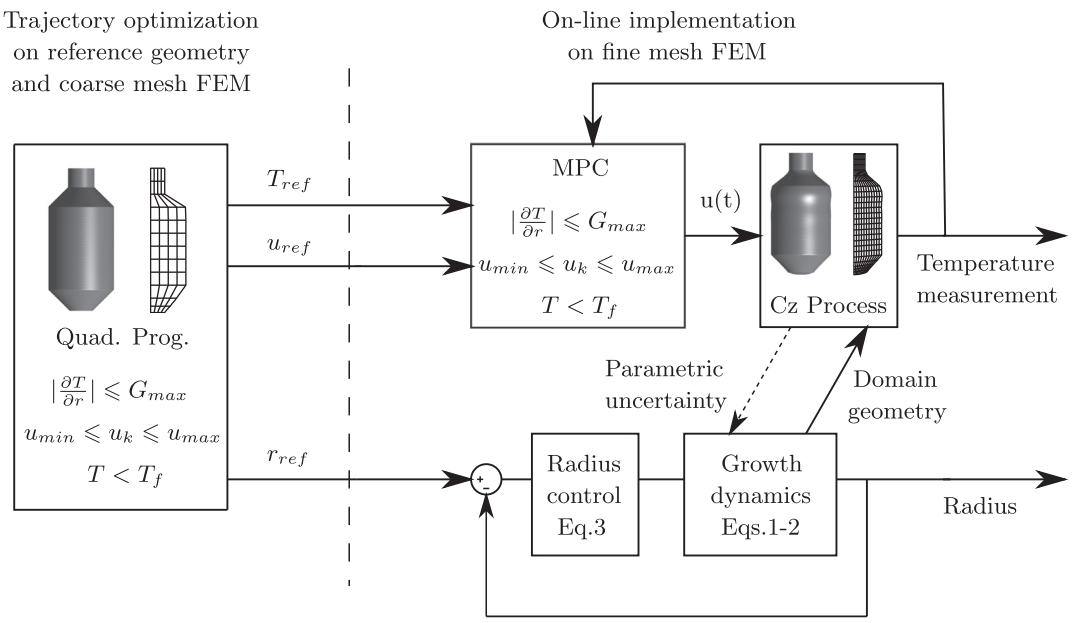

Fig. 3. Trajectory optimization and temperature distribution control algorithm along with the coupling between pulling and heat transfer dynamics. Two-way coupling is reduced to one-way coupling by considering the effect of thermal phenomena on crystal shape as an uncertainty in crystal growth rate.

crystal consist of a parabolic PDE model Eq. (9) along with time-varying boundary conditions Eqs. (6)–(8) which are coupled to pulling dynamics given by Eq. (1).

2.3. Thermal stresses in crystal

Crystal dislocations are generated by thermally induced stresses during the process and suppression of significant thermal stresses results in reduced dislocation density in the produced crystal. Temperature gradients are known to be the source of thermal stresses and is one of important factors in creating dislocations in the crystal. Obtaining exact thermal stresses in the crystal during the crystallization process requires detailed modelling of the coupled thermal, growth phenomena and meniscus dynamics. In order to circumvent complex modelling there are existing useful conservative criteria on temperature gradients which imply keeping stresses to exceed the critical values.

The thermal stress in the crystal can be calculated with the assumption of plain strain in the crystal to define the aforementioned criteria for temperature gradients (Gevelber, 1994). The stresses are at their maximum values at the crystal center and the crystal surface. Assuming plain strain and a simple meniscus geometry, Gevelber (1994) provided these stresses as temperature dependent functionals given by:

$$\sigma_{r,norm} = \begin{cases} -\frac{5}{48}\frac{\partial T}{\partial r}R_c & \text{at } r = 0 \\ 0 & \text{at } r = R_c \end{cases} \tag{10}$$

$$\sigma_{z,norm} = \begin{cases} -\frac{10}{48}\frac{\partial T}{\partial r}R_c & \text{at } r = 0 \\ \frac{7}{24}\frac{\partial T}{\partial r}R_c & \text{at } r = R_c \end{cases} \tag{11}$$

$$\sigma_{\theta,norm} = \begin{cases} -\frac{5}{48}\frac{\partial T}{\partial r}R_c & \text{at } r = 0 \\ \frac{7}{24}\frac{\partial T}{\partial r}R_c & \text{at } r = R_c \end{cases} \tag{12}$$

The maximum stress is obtained in the growth direction and stresses are the largest at the crystal surface and they should be less than critical resolved shear stress (σ_{CRSS}). For Silicon crystal, the critical stress is $\sigma_{CRSS} = 5.55 \times 10^6$ dyn/cm^2 and this condition is reduced to Gevelber (1994):

$$|\frac{\partial T}{\partial r}|R_c \begin{cases} \leq 10.3\,\text{K for } r = R_c \\ \leq 28.8\,\text{K for } r = 0 \end{cases} \tag{13}$$

Since the maximum stress occurs at the crystal surface, the temperature gradients should be the minimum at the crystal surface. The constraints on the temperature gradients are considered to be less than the maximum value at the crystal surface. The temperature gradient at points far from the interface are not important in creating dislocations and therefore the constraints are considered only on the elements in the proximity of the melt–crystal interface.

3. Optimization and temperature reference tracking

The conduction–convection heat transfer model provided in Section 2.2 is used for process optimization and control. Since the crystal shape is not known at the beginning of the process, the reference crystal shape (reference crystal radius and length) is used for trajectory planning and optimization. The heater input $Q(t)$ is determined such that the maximum cooling is achieved and the constraints on the input and the temperature gradients close to melt-crystal interface are not violated. Hence, optimization on the reference crystal shape is plausible since the radius control law is robust with respect to uncertainty in growth rate which results from temperature distribution within the crystal. A low dimensional finite element model of the crystal as the dynamic model along with quadratic programming are used to determine the heater inputs optimizing the objective function and satisfying the constraints. The optimization and control framework used in this article is shown in Fig. 3.

The presence of non-trivial crystal shape, moving boundaries and actuation being placed at one boundary makes available options for model base reduction and process control quite limited. In order to address model and controller design complexities in this work, we developed finite element model (FEM) of the process model which is used for optimization and controller synthesis. The

FEM model of the conduction–convective PDE given by Eqs. (8) and (9) can be cast in the following form:

$$X_{k+1} = A_k X_k + B_k u_k + Bc_k,\ X(0) = X_0$$
$$Y_k = C_k X_k \tag{14}$$

where X_k is the vector of temperature field at nodes of FEM model at kth time instance, $k = 0, 1, 2, \ldots$, A_k and B_k are the time-varying matrices obtained from FEM and Bc_k term is associated with Dirichlet boundary conditions at the crystal surface, $u_k = Q_k/Pe$ is the heater input to the system. The system output, Y_k, defines the temperature gradients at nodes of interest. Due to the moving boundaries and time varying term in the PDE, the dynamical system given by Eq. (14) is time-varying.

Knowing the reference crystal shape, the finite element method is used to optimize the temperature distribution evolution for the batch process time. The optimal inputs are obtained such that the maximum cooling takes place without violating the temperature gradients. The most important gradients are those close to the melt-crystal interface and since the radial gradients at the inner boundary are zero (boundary condition at $r = 0$, $\partial x/\partial r = 0$), the gradients inside the crystal are appropriately taken into account. In order to obtain an optimal temperature trajectory, the following optimization problem is solved to maximize cooling of the crystal by keeping the temperature gradients within the desired level.

$$\min_{u1,\ldots,u_{N_p}} J = \sum_{k=1}^{N_p} X_k^T Q X_k + u_k^T R u_k \tag{15}$$

subject to:

$$X_{k+1} = A_k X_k + B_k u_k + Bc_k \tag{16}$$

$$u_{\min} \le u_k \le u_{\max} \tag{17}$$

$$|Y_k| \le G_{\max} \tag{18}$$

where N_p is the number of time intervals used to span time duration of the whole crystal growth process. In order to solve the optimization problem, one can formulate a large-scale quadratic program with known evolution of the system matrices (A_k, B_k and Bc_k). The reference crystal shape evolution is utilized to generate FEM matrices for entire process time and consequently these matrices are used to formulate the quadratic program. The optimal trajectory is obtained by solving the quadratic program, Eqs. (15)–(18) and is utilized as the reference trajectory for temperature tracking control of the process.

Knowing the optimal reference trajectory, model predictive reference tracking control is used to track the reference trajectory by measuring crystal temperature at the crystal surface. Model predictive control uses the finite element model of the process to predict future behaviour of the process and optimize the input such that the control action keep the process close to the reference trajectory. For temperature tracking, the model predictive reference tracking is defined as:

$$\min_{u_0 \ldots u_{N_c-1}} \Phi = \sum_{k=1}^{N_c} (y_k^r - C_k' X_k)^T Q' (y_k^r - C_k' X_k) + \sum_{j=0}^{N_c-1} (u_k - u_k^r)^T R' (u_k - u_k^r) \tag{19}$$

subject to:

$$X_{k+1} = A_k X_k + B_k u_k + Bc_k \tag{20}$$

$$y_k = C_k' X_k \tag{21}$$

$$u_{\min} \le u_k \le u_{\max} \tag{22}$$

$$|Y_k| \le G_{\max} \tag{23}$$

where y_k^r and u_k^r are the reference trajectory and reference inputs at time instance k, obtained from optimization problem (Eqs. (15)–(18)) and $y_k = C_k' X_k$ is the temperature measurement at the crystal surface. Q' and R' are positive definite penalty matrices.

The trajectory obtained from the finite element model (Eq. (14)) is used as reference trajectory. Then MPC reference tracking controller is constructed using the on-line crystal shape (not reference geometry) to track the temperature reference. The temperature gradient constraints are present in the MPC formulation to avoid high gradients in the crystal. The integrated control and optimization is shown in Fig.1. Therefore, the controller realization is given by two steps, first by calculation of the optimal inputs along with optimal temperature trajectories which takes into account all present constraints. Then by optimal temperature trajectory and more refined finite element model on the tracked crystal shape, reference temperature tracking is performed. Since the finite element model used for MPC is different than the model used for optimization (different crystal shape and non-planar interface), there is a necessity to have temperature gradient constraint present in the MPC synthesis as ultimate tool of process regulation.

4. Numerical simulation results

The reference temperature tracking provided in this paper is based on the FEM model of heat transfer in Czochralski crystal growth process. The temperature distribution evolution optimization is performed on a pre-defined reference crystal shape. Then the temperature tracking is provided using the optimal temperature trajectory obtained on the reference crystal shape and the model predictive reference temperature tracking is implemented on the high fidelity FEM model of the temperature evolution on the realistic crystal shape in the presence of disturbances in the model (see Fig. 3).

Two finite element model of the process are used. The first is a low dimensional model with DOF of 80 (5×16 two-dimensional linear 4-node elements) for off-line optimization given by Eqs. (15)–(18). This finite element model is constructed on the reference crystal geometry with planar interface and utilized for off-line optimization. The second realized and constructed finite element model has 348 DOF (12×29 two-dimensional linear 4-node elements) which is build on the basis of realistic crystal geometry with non-planar interface and is utilized as the process model to verify the proposed control design. The FE models are derived on the crystals with non-cylindrical and time-varying domain where the crystal domain movement (time evolution of the radius and length $R_{c.i.}(t)$ and $l(t)$) are obtained from reference crystal shape for the former and the on-line coupled implementation of the radius control (Eqs. (3) and (4)) for the latter. Note that the spatial domain of the crystal is known from pulling dynamics and therefore the Arbitrary Lagrangian Eulerian (ALE) method (Reddy, 2004) is used to discretize the spatial domain of the crystal. First-order implicit time integration with the time step $dt = 0.005$ is used to obtain the evolution of the time-varying system.

The control synthesis, introduced in Section 2, is used to track the reference crystal radius. The control law given in Eq. (3) is used to control the crystal shape, however due to the present uncertainty, the tracked crystal geometry is slightly different than the reference shape. The reference crystal radius as a function of crystal length along with 3-D representation of the reference and tracked crystal geometry are shown in Fig. 4. The tracking performance of controller is shown as dash-dotted line. The reference crystal geometry (Fig. 4, left side crystal shape) is known and used as the crystal geometry for temperature distribution evolution optimization and trajectory calculation. The obtained inputs and trajectories are implemented on the realistic crystal shape Fig. 4, right side crystal shape) crystal geometry.

Since the desired crystal shape evolution is known and can be arbitrarily pre-specified, the time-varying evolution of the crystal

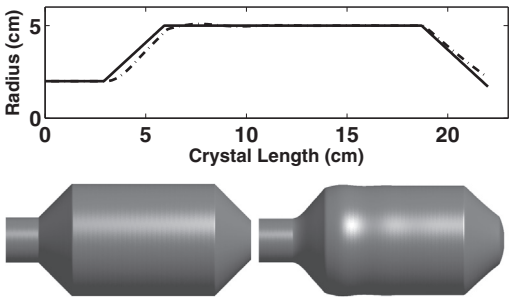

Fig. 4. The reference crystal shape (solid line) and the tracked crystal radius (dash-dotted line) – the 3-D reference crystal shape along with the tracked 3-D crystal.

mesh can be obtained from the reference crystal shape for the whole crystal processing time. Using the known time-varying mesh, the system dynamics is represented by FE model (Eq. (14)). The crystal is assumed to be at equilibrium at the beginning of the process (temperature distribution initial condition) and the quadratic programming (QP) is used to optimize the inputs and the temperature distribution evolution throughout the process. In order to implement the QP, the total crystal growth process time is considered to be 3.5 h with average crystal growth of 5 cm/h. The dynamic model is discretized using sampling time of 26 s which results in 500 manipulating variables in QP framework to be optimized. A FE model with DOF of 70 is used for optimization which results in 35000 equality constraints along with more than 35,000 inequality constraints at nodal temperatures in QP realization.

The MPC is implemented on the more realistic FE model of the process with non-planar interface and in presence of model disturbance of white noise with the covariance of 10% of the maximum temperature. The reference input along with inputs generated by MPC are shown in Fig. 5a and the reference trajectory along with tracked temperature are shown in Fig. 5b. As it can be seen the MPC tracks the reference temperature trajectory with high accuracy at the beginning of the process. However the tracking efficiency decreases (maximum deviation of 2%) as the crystal grows and the distance between the actuation and the point of interest increases. In absence of disturbances the MPC follows the reference with deviation less than 0.1%. A proportional-integral (PI) controller is realized for comparison purpose and the input and tracked temperature generated by PI controller are presented along with MPC results in Fig. 5. The PI controller tracks the reference trajectory, however, the constraints on minimum heater input and maximum temperature are violated. Moreover, PI controller only tracks the temperature evolution at the measurement point and the

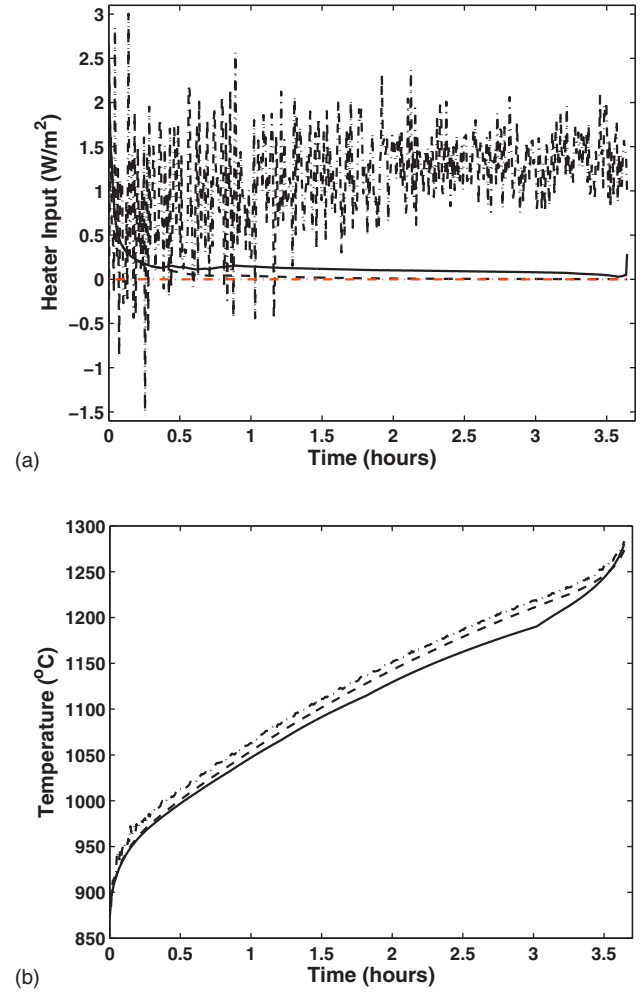

Fig. 5. Reference input and temperature trajectory located on the seed crystal surface (solid lines) along with the input and tracked temperature by MPC (dashed lines) and PI controller (dash-dotted lines). The red line, constant dashed line at zero, shows the minimum heater input constraint.

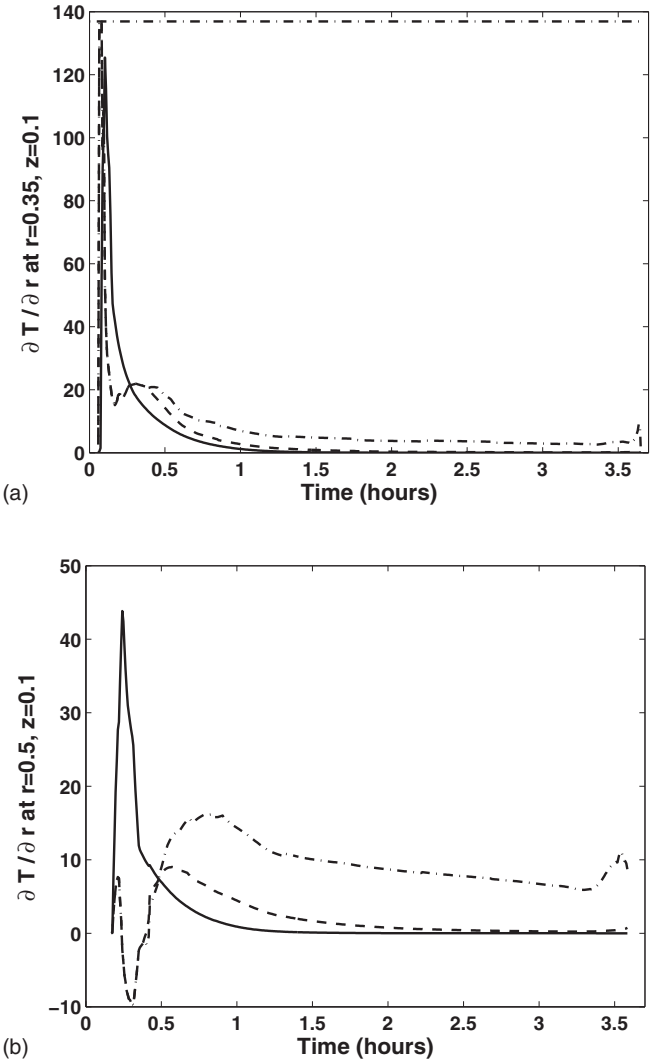

Fig. 6. Radial temperature gradients at points close to melt-solid interface, gradient unit is °C/m. Temperature trajectory located at the seed crystal surface (solid lines) along with the input and tracked temperature by MPC (dashed lines) and PI controller (dash-dotted lines).

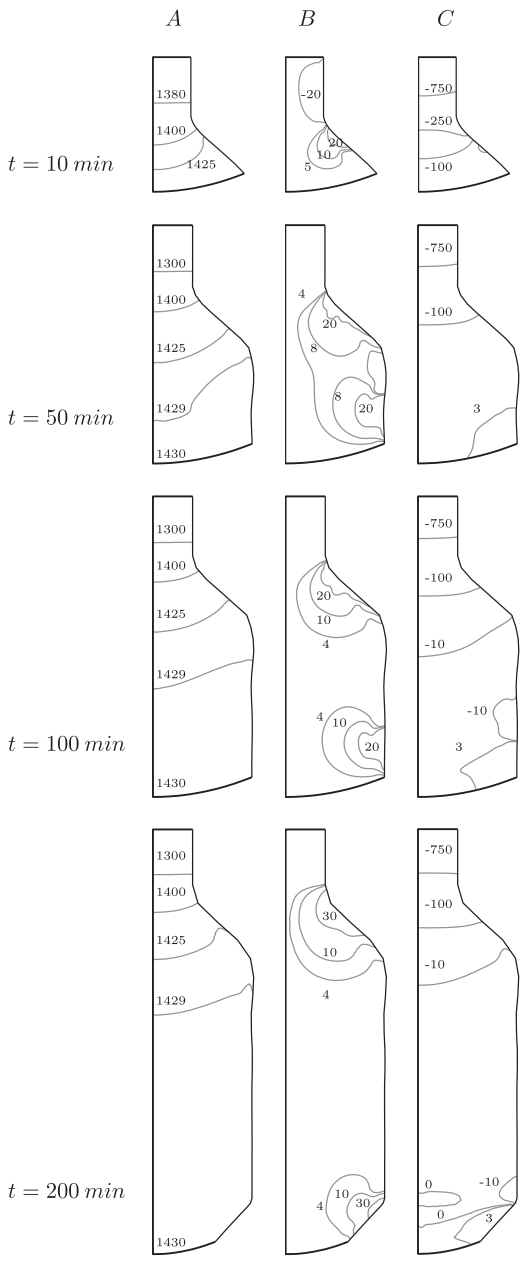

Fig. 7. Temperature and gradients distribution in the crystal at different time instances. (A) Temperature distribution, °C; (B) radial gradients, °C/m; and (C) longitudinal gradients, °C/m.

temperature distribution within the solid crystal is not tracked very well (see Movie 1). The reference temperature distribution trajectory along with tracked temperature distributions by MPC and PI controller are shown in Movie 1.

Temperature gradients for few points within the crystal are shown in Fig. 6 along with the temperature distribution and temperature gradient contours in Fig. 7 and as it can be seen, despite the fact that the constraints are not active all the time, the constraints on the maximum temperature gradient in both radial and longitudinal directions are satisfied. Temperature gradients in longitudinal direction are very large at points far from the interface (solidification interface) as the heater actuation flattens the temperature distribution at points closer to the interface to avoid large gradients in this region. The radial gradients have more crucial effect on the crystal quality and they are compensated (see Fig. 7). Along this line, one can also inspect the overall temperature and spatial gradients evolution during the growth process under the MPC reference tracking trajectory regulation. Movie 2 demonstrates successful MPC controller design and implementation.

5. Summary

The reference temperature distribution tracking problem is considered in this work. Temperature tracking is performed by tracking a desired point temperature evolution along with satisfying the present constraints. The optimal temperature trajectory is obtained using quadratic programming and then the MPC is implemented to control the coupled pulling dynamics and conduction-convection heat transfer model. The provided approach in this work uses a simplified model of heat transfer in Czochralski crystal growth process that preserves the main effect of temperature dynamics and the thermal behaviour of the Czochralski process, however, the approach can be extended to more comprehensive model by including the heat radiation, the heater/actuator dynamics and also the heat transfer in fluid and meniscus in both the optimization and implementation steps. It is demonstrated that tracking the predetermined optimal reference trajectory is a reliable way to maximize cooling efficiency which can be applied to different settings to achieve a desired goal of minimizing thermal stresses during the crystallization process.

Acknowledgements

The authors thank the anonymous reviewers for their valuable comments and suggestions to improve the quality of the article. Financial support by Natural Science and Engineering Research Council of Canada (NSERC) Discovery Grant 386508-2011 is gratefully acknowledged.

Appendix A. Supplementary Data

Supplementary data associated with this article can be found, in the online version, at http://dx.doi.org/10.1016/j.compchemeng.2014.09.005.

References

Abdollahi J, Dubljevic S. Crystal radius and temperature regulation in Czochralski crystallization process. In: Proceedings of the American control conference; 2013. p. 1626–32.
Abdollahi J, Izadi M, Dubljevic S. Temperature distribution reconstruction in Czochralski crystal growth process. AIChE J 2014, DOI 10.1002/aic.14486.
Armaou A, Christofides P. Crystal temperature control in Czochralski crystal growth process. AIChE J 2001a;47(1):79–106.
Armaou A, Christofides PD. Robust control of parabolic PDE systems with time-dependent spatial domains. Automatica 2001b;37:61–9.
Cao J, Gao Y, Chen Y, Zhang G, Qiu M. Simulation aided hot zone design for faster growth of Cz silicon mono crystals. Rare Met 2011;30(2):155–9.
Demina S, Kalaev V. 3D unsteady computer modeling of industrial scale Ky and Cz sapphire crystal growth. J Cryst Growth 2011;320(1):23–7.
Derby J, Brown R. On the dynamics of Czochralski crystal growth. J Cryst Growth 1987;83(10):137–51.
Fang H, Qiu S, Zheng L, Schaffers K, Tassano J, Caird J, et al. Optimization of the cooling profile to achieve crack-free Yb:S-FAP crystals. J Cryst Growth 2008;310(16):3825–32.
Gevelber M. Dynamics and control of the Czochralski process: III. Interface dynamics and control requirements. J Cryst Growth 1994;139(3-4):271–85.
Gevelber M, Stephanopoulos G. Dynamics and control of the Czochralski process: I. Modelling and dynamic characterization. J Cryst Growth 1987;84(4):647–68.
Gevelber M, Stephanopoulos G, Wargo M. Dynamics and control of the Czochralski process: II. Objectives and control structure design. J Cryst Growth 1988;91(1/2):199–217.
Irizarry-Rivera R, Seider WD. Model-predictive control of the Czochralski crystallization process: Part I. Conduction-dominated melt. J Cryst Growth 1997;178(4):593–611.
Lee K, Lee D, Park J, Lee M. MPC based feedforward trajectory for pulling speed tracking control in the commercial Czochralski crystallization process. Int J Control Autom Syst 2005;3(2):252–7.

Neubert M, Winkler J. Nonlinear model-based control of the Czochralski process: III. Proper choice of manipulated variables and controller parameter scheduling. J Cryst Growth 2012;360(1):3–11.
Ng J, Aksikas I, Dubljevic S. Control of parabolic PDEs with time-varying spatial domain: Czochralski crystal growth process. Int J Control 2013;86(9):1467–78.
Ng J, Dubljevic S. Optimal boundary control of a diffusion–convection–reaction PDE model with time-dependent spatial domain: Czochralski crystal growth process. Chem Eng Sci 2012;67:111–9.
Reddy JN. An introduction to nonlinear finite element analysis. Oxford University Press; 2004.
Rudolph J, Winkler J, Woittennek F. Flatness based approach to a heat conduction problem in a crystal growth process. In: Meurer T, Graichen K, Gilles ED, editors. Control and observer design for nonlinear finite and infinite dimensional system. Springer Verlag; 2005. p. 387–401.
Sinno T, Brown R. Modeling microdefect formation in Czochralski silicon. J Electrochem Soc 1999;146(6):2300–12.
Sinno T, Dornberger E, von Ammon W, Brown R, Dupret F. Defect engineering of Czochralski single-crystal silicon. Mater Sci Eng R 2000;28(5-6):149–98.
Winkler J, Neubert M, Rudolph J. Nonlinear model-based control of the Czochralski process: I. Motivation, modeling and feedback controller design. J Cryst Growth 2010a;312:1005–18.
Winkler J, Neubert M, Rudolph J. Nonlinear model-based control of the Czochralski process: II. Reconstruction of crystal radius and growth rate from the weighing signal. J Cryst Growth 2010b;312:1019–28.
Winkler J, Neubert M, Rudolph J. A review of the automation of the Czochralski process. Acta Phys Pol A 2013;124:181–92.